FREE FIELD VIBRATIONS DUE TO PILE DRIVING USING A COUPLED FEM WITH SBFEM METHOD

Kuo-Feng Lo [1], Sheng-Huoo Ni [2], Yan-Hong Huang [1], and Lutz Lehmann [3]

ABSTRACT

This paper presents a three-dimensional numerical model for the prediction of free field vibrations due to the vibratory and impact of pile driving. A new coupling methodology, finite element method (FEM) with scaled boundary finite element method (SBFEM), has been adopted to simulate the pile driving process into a layered ground. With this numerical model, the reflection energy can be absorbed on the near-/far-field interface without accuracy reduction, while simulation time and amount are reduced. The results indicate that the ground surface vibration during piling will not be affected while the receiver is located away from source over than five times of pile diameter with vibration frequency fixed at 20 Hz.

Key words: Vibration, soil-pile-interaction, SBFEM, pile driving.

1. INTRODUCTION

Ground surface vibrations are generated either by human activities, traffic loading, construction induced, *etc*. The common man-made vibrations are caused by pile driving, blasting, *etc*. The analyzed pile is a large displacement driving pile, which is fabricated prior to installation and then driven into the ground by impact or vibratory hammers. Frequently, vibrations produced during construction operations became a concern since they can disturb people and cause some damage on adjacent structures, where the induced vibrations may cause cracks in the walls or in the facade. During the pile driving, the energy transmitted through the soil is very high and causes large soil deformations and settlements in the near-field. In the far field, reported data show that the induced vibrations cause deformations in the elastic range (Kim and Lee 2002). So, the deformation at a certain distance to the pile can be assumed to have a linear elastic constitutive behavior in the unbounded soil. The approach has been used in the finite element method (FEM) simulations of To and Smith (1988), and Mabsout (1999). With these FEM analyses, the effects of different driving methods on the surrounding soil are able to be predicted. Nevertheless, FEM models can perform well in non-homogeneous and anisotropic materials for non-linear material behaviour and complex geometry of a structure. However, the dynamic response of unbounded (or semi-infinite) medium model can not be simulated for a vast spatial discretisation. As common transmitting boundaries, like simple spring-dashpots, are generally only approximate representations of the unbounded soil located on the artificial boundaries' exterior, certain reflections will occur. Obviously, FEM cannot satisfy the boundary conditions at infinity exactly. The spatial discretisation is terminated on an artificial boundary where the truncated domain outside the boundary up to infinity can only be represented approximately. The important factors affecting the accuracy of the modelled response of a structure by FEM are the type of the transmitting boundary and its distance from the structure. In other words, it is to be expected that the farther away the artificial boundary is placed, the more accurate the results become.

The use of infinite elements (IE) to model continua has been developed particularly by Bettess (1992). This method is very effective in preventing spurious reflection when a single wave type at a defined transmission velocity strikes the artificial boundary. However it is less effective when the wave pattern contains components of different velocities. Further difficulties may arise if static forces such as self-weight are applied prior to the dynamic analysis (Ramshaw and Selby 2003). The scaled boundary finite element method (SBFEM) was developed for bounded and unbounded domains over the past few years addressing elastodynamics and diffusion (Wolf 2003). Main application of the SBFEM is the analysis of wave propagation problems in an elastic half-space, occurring in soil- structure interaction simulations in time and frequency domain. SBFEM performs well in calculating the dynamic stiffness matrix for both homogeneous and non-homogeneous discretised mediums, which extend to infinity and it does not require a fundamental solution as the boundary element method (BEM). Coupling the SBFEM to the FEM has been proved to reduce the computational effort for long simulation times dramatically, while the accuracy of the model is not affected (Lehmann 2005).

As the focus is on the response in the far field, where deformations are relatively small, a linear elastic constitutive behavior is assumed for the soil. The free field vibrations are calculated by means of a coupled FE-SBFEM model using a subdomain formulation. The vibratory pile driving is modeled, where the vibration frequency is fixed at 20 Hz for different penetration depths. Herein, the pile and the soil (near-field) modeled by the FEM and the unbounded soil (far-field) by SBFEM. The ground surface vibrations are observed at several distances from pile centre, 2D, 5D and 10D, where D is pile diameter.

Manuscript received November 26, 2011; revised August 12, 2012; accepted August 20, 2012.

[1] Ph.D. student, Department of Civil Engineering, National Cheng-Kung University Tainan, Taiwan.

[2.] Professor (corresponding author), Department of Civil Engineering, National Cheng-Kung University Tainan, Taiwan. (e-mail: tonyini@mail.ncku.edu.tw).

[3.] Senior Lecturer, Institute of Applied Mechanics, Technical University of Braunschweig; Germany.

2. COUPLED FEM/SBFEM

The SBFEM (Wolf 2003) based on the FE formulation and satisfies the radiation condition at infinity while reducing the spatial dimension by one. The solution is analytical in the radial direction while the solution in the circumferential direction is approximative in the sense while it converges to the exact solution as the number of degrees of freedom increases. As discussed above, the FEM is chosen to map the near-field while the SBFEM is utilized to absorb the reflection energy at the artificial boundary. Such a hybrid method has some unique features:

1. Reduction of one spatial dimension without requiring a fundamental solution.
2. No discretisation of free and fixed boundaries and interfaces between different materials in the sound domain.
3. Influence of the infinite far-field could be stored in the form of influence matrices for further simulations (different near-field geometries or load cases).
4. Straightforward incorporating in existing FEM codes and concise coupling with FEM.

2.1 Governing Equation

A summary of the governing equations of linear theory to the time domain is given. The Hooke's law with the vector of strain states can simply be displayed as:

$$\boldsymbol{\sigma} = \mathbf{D}\boldsymbol{\varepsilon} \tag{1}$$

where $\sigma^T = [\sigma_x\ \sigma_y\ \sigma_z\ \tau_x\ \tau_y\ \tau_z]$, is the stress vector and

$\varepsilon^T = [\varepsilon_x\ \varepsilon_y\ \varepsilon_z\ 2\varepsilon_{xy}\ 2\varepsilon_{xz}\ 2\varepsilon_{yz}]$, is the vector containing the (compressing) strain states.

D is the elasticity matrix which may be stated for isotropic or anisotropic material.

For linear theory, the strain tensor is defined by the strain-displacement relationship

$$\boldsymbol{\varepsilon} = \mathbf{L}\mathbf{u} \tag{2}$$

With the differential operator **L** given in its transposed form by:

$$\mathbf{L}^T = \begin{bmatrix} \frac{\partial}{\partial x} & 0 & 0 & \frac{\partial}{\partial y} & \frac{\partial}{\partial z} & 0 \\ 0 & \frac{\partial}{\partial y} & 0 & \frac{\partial}{\partial x} & 0 & \frac{\partial}{\partial z} \\ 0 & 0 & \frac{\partial}{\partial z} & 0 & \frac{\partial}{\partial x} & \frac{\partial}{\partial y} \end{bmatrix}. \tag{3}$$

Applying this operator (Eq. (3)) on $\boldsymbol{\sigma}$, the equation of motion in the time domain is given by:

$$\mathbf{L}^T\boldsymbol{\sigma}(t) + \mathbf{b}(t) - \rho\ddot{\mathbf{u}}(t) = \mathbf{0}\ , \tag{4}$$

where ρ means the material density; the stresses $\boldsymbol{\sigma}(t)$, body forces $\mathbf{b}(t)$, and displacements $\ddot{\mathbf{u}}(t)$ are time-dependent.

2.2 Hybrid FEM/SBFEM Scheme

Equation (4) represents the equation of motion in the time domain for a general case. The analyzed domain can be divided into two parts: Near- / far-field as shown in Fig. 1. A time-dependent interaction force vector $\mathbf{r}_b(t)$ on the interface between near-field and far-field is introduced. Then introducing the γ-parameter of the Hilber-Hughes-Taylor implicit time integration scheme (Hilber *et al*. 1997), the equation of motion can be written as (Crouch and Bennet 2000):

$$\begin{bmatrix} \mathbf{K}_{ss} & \mathbf{K}_{sb} \\ \mathbf{K}_{bs} & \mathbf{K}_{bb} \end{bmatrix} \begin{bmatrix} \mathbf{u}_s(t) \\ \mathbf{u}_b(t) \end{bmatrix} + \begin{bmatrix} \mathbf{M}_{ss} & \mathbf{M}_{sb} \\ \mathbf{M}_{bs} & \mathbf{M}_{bb} + \gamma\Delta t\mathbf{M}_0^{\infty} \end{bmatrix} \begin{bmatrix} \ddot{\mathbf{u}}_s(t) \\ \ddot{\mathbf{u}}_b(t) \end{bmatrix} = \begin{bmatrix} \mathbf{P}_s(t) \\ \mathbf{P}_b(t) - \mathbf{r}_b(t) \end{bmatrix} \tag{5}$$

where the mass matrix **M**, the stiffness matrix **K**, and the node value vectors of the displacements **u** and accelerations $\ddot{\mathbf{u}}$, respectively, are subdivided corresponding to the location of the nodes, *i.e.*, subscript *b* denotes the nodes on the soil-structure interface and the subscript *s* the remaining nodes of the structure. On the right hand side of Eq. (5) $\mathbf{P}(t)$ is the vector of external forces and $\mathbf{r}_b(t)$ represents the interaction forces between the near- and far-field. When the interaction force vector $\mathbf{r}_b(t)$ is determined, the dynamic response of the structure can be obtained from Eq. (5) by using direct integration schemes, such as the Hilber-Hughes-Taylor implicit time integration scheme.

In the substructure method, the interaction forces on the near-field/far-field interface are given by the convolution integral

$$\mathbf{r}_b(t) = \int_0^t \mathbf{M}_{\infty}(t-\tau)\ \ddot{\mathbf{u}}_b(\tau)\ d\tau \tag{6}$$

where $\mathbf{M}_{\infty}(t)$ is the acceleration unit-impulse response matrix of the soil at a node which will subsequently lie on the near-field/far-field interface. The calculation of convolution integral (6) is computational expensive for long simulation times. Hence, a reduction of non-locality in time, as suggested by Lehmann (2004, 2005) is used.

The derivation of the SBFEM and its solution procedures are discussed in Wolf and Song (2000). In the scaled boundary finite element method, a so-called scaling centre is chosen in a zone from which the total boundary, other than the straight free surface passing through the scaling centre, must be visible as shown in Fig. 1. Only the boundary visible from the scaling centre is discretized. The coordinates of the nodes of an element in the three-dimensional Cartesian coordinate system are arranged in $\{x\}\{y\}\{z\}$ (Fig. 2). The geometry of the near-/far field interface is described by a finite element discretization with local coordinates η,ζ on the boundary (Wolf and Song 1996). The governing differential equations are transformed to this coordinate system. Two dimensional finite elements represent the far-field/near-field interface of a three-dimensional problem, while a radial coordinate ξ contains the scaling factor. The axes η and ζ lay in the circumferential directions (on the boundary). As shown in Fig. 2 for an unbounded

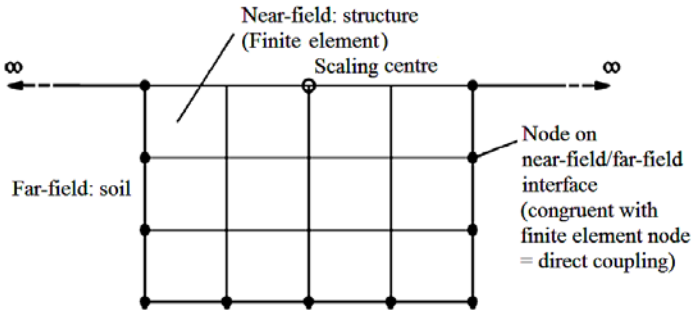

Fig. 1 Discretisation scheme of soil-structure-interaction system (Lehmann 2005)

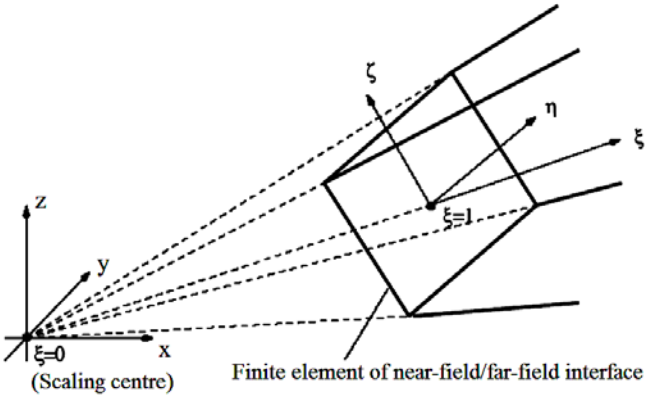

Fig. 2 Finite element and 3D coordinate system of scaled boundary transformation (Lehmann 2005)

medium, the radial coordinate ξ points from the boundary towards infinity where the boundary condition at infinity (radiation condition) can be incorporated in the analytical solution. The change of coordinates from Cartesian coordinate system to the scaled boundary coordinates ξ, η and ζ is called the scaled boundary transformation. It means that the governing differential equations can be solves in the radial direction analytically and in the circumferential directions numerically. Hence, the method reduces the governing partial differential equations (PDE) to a set of ordinary differential equations (ODE). This is achieved by introducing finite element shape functions in the circumferential direction and solving the ODE thus formed analytically in the normalized radial direction. More details about boundary discretization and dynamic-stiffness matrix can be found in Wolf and Song (1996); Wolf (2003).

Initially, to perform a scaled boundary formulation, one has to discretise the boundary with finite elements. Applying the scaled boundary transformation and Galerkin's weighted residual method, the governing partial differential equations are reformulated as the SBFE equation in displacement (solids), with the radial coordinate as independent variable. For a time domain analysis a further transformation is mandatory. A final numerical discretisation allows to use the computer-based analyses.

3. NUMERICAL MODEL

The free field vibrations due to driving of a concrete pile in a semi-infinite medium are investigated. The majority of modern pile vibrators perform at frequencies, ranging typically between 20 to 40 Hz. Modern vibrators can generate a force up to 4000 kN. As the responses of ground surface vibration amplitude are relatively small, a linear elastic constitutive behavior is assumed for the soil. A vibratory pile driver operates by continuously shaking the pile at a fixed frequency to vibrate the pile into the ground. In this paper, the pile and its surrounding soil is modeled to simulate the pile driving process with a fixed vibration frequency at 20 Hz. The pile driving force will generate a sinusoidal force with the amplitude of 1000 kN and period of 0.1 second during pile installation. The pile has a length 20 m, a diameter 0.6 m, a Young's Modulus E_p = 4000 MPa, a Poisson's ratio v_p = 0.2, and a density ρ_p = 2400 kg/m^3. The pile and the soil are modeled using 8-node brick elements; with a linear elastic material behaviour. In this model, the total node number is 3929 and the element number is 3696. The minimum element length is 0.3 m, maximum element is 15.3 m and the maximum distance from pile centre to the near-/far-field interface is 12 times pile diameter (13D, where D is the pile diameter). However, to avoid the unknown influence by the interface of the near-/far-field, the maximum discussed distance is 10D, which far from the pile centre. A time step Δt = 0.002 for 12.0 seconds are used for the time-domain simulation.

The subsoil conditions are based on the subsoil exploration (up to 20.0 m depth) drilled in a construction site (Ni and Chuang 2001). The soil strata are defined as 4 layers and bedrock. Their properties are soft clay and loose to medium dense sands as shown in Table 1. Poisson's ratio (v_s) of all soil layers are assumed to be 0.3. The bottom soil (below 20 m) is the bedrock. In the numerical model, the bedrock is considered as fixed boundary conditions at the bottom of the FE domain.

4. RESULTS AND DISCUSSIONS

4.1 Investigation of Several Penetration Depths

Ground surface vibrations due to operating frequency of piling f_p = 20 Hz are considered during processing. The vibrations of the ground surface are discussed in the distance range d = 1D – 10D to the pile centre. The results of various pile driving depths are shown in Fig. 3. In Fig. 3(a), the pile is installed in the subsoil at the depth 1.3 m. The maximum amplitude (3.5×10^{-7} m at t = 0.0s) occurs at the position 2D, then decays as time greater than 1.3s. The vibration amplitudes

Table 1 Soil property parameters in the numerical model

Depth (m)	Soil Classification	Submerged Unit Weight γ' (kN/m^3)	Young's Modulus E_s (kN/m^2)
0 ~ 2.6	Soil 1: CL	8.61	20000
2.6 ~ 7.4	Soil 2: SM	10.39	55000
7.4 ~ 12.0	Soil 3: CL	9.27	20000
12.0 ~ 20.0	Soil 4: SM	9.29	65000
> 20	Bedrock	–	–

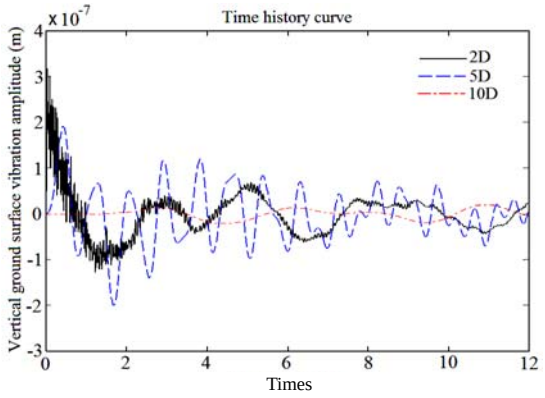

(a) Pile driving depth at 1.3 m

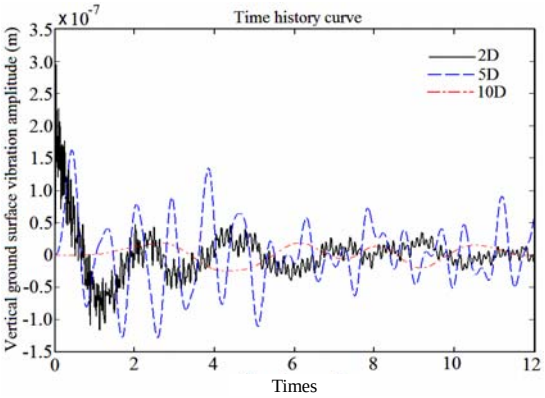

(b) Pile driving depth at 5 m

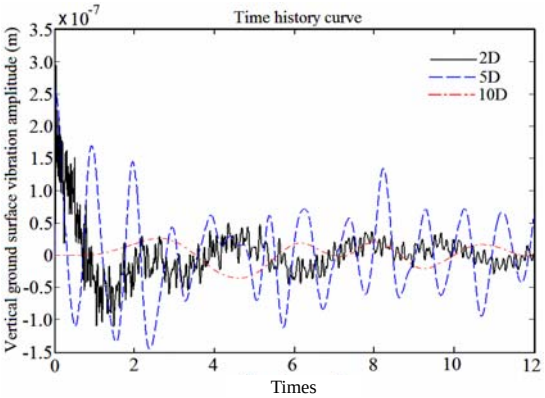

(c) Pile driving depth at 9.7 m

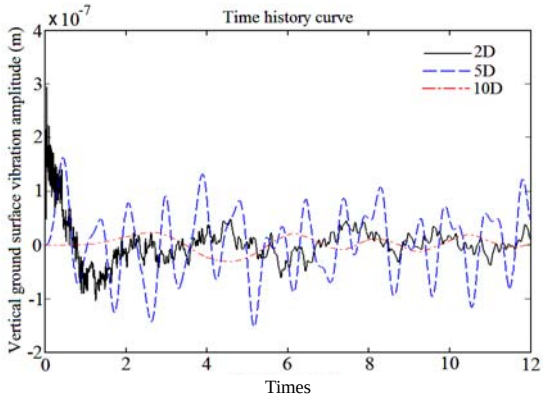

(d) Pile driving depth at 16.0 m

Fig. 3 The time history curve of vertical displacement on the ground surface with pile driving depth at (a) 1.3 m (b) 5.0 m (c) 9.7 m (d) 16.0 m

are between -1.3×10^{-7} to 0.2×10^{-7} m between t = 2 to 12s. As to d = 5D, it is an analogous-harmonic vibration, the amplitude is between -2×10^{-7} and 2×10^{-7} m, and without distinctive decay tendency in the curve until t = 12s with tremors. As regards to d = 10D, the vibration amplitude is smaller relatively between -2×10^{-8} and 2×10^{-8} m, and the curve is smoother than the others. Figures 3(b) to 3(d) show the results of pile driving depths in the 5 m, 9.7 m and 16 m, respectively. Comparing the results of Figs. 3(a) ~ 3(d), there is no difference in the position of peak amplitude of curve 2D. All the curves have higher oscillations (or noise) during the whole simulation time. The main reason is that the receiver position 2D is too close to the pile and the its vibration affects the ground surface vibration seriously.

Concerning the distances 5D, the curves look similar and the main amplitudes are below 1.5×10^{-7} m. In addition, there is agreement in all curves 10D and they keep small and smooth vibrations during the whole time. Hence, it can be summarized that the different subsoil properties do not affect the vibration amplitude with any significance even the pile driving depth is at different soil layers. But the factor of d affects the vibrations a lot, the distance is farther and the amplitude is smaller.

4.2 Distances from Pile Centre

Test results of three different receivers located at 2D, 5D and 10D on the ground surface are discussed while the pile driving depth are into different soil layers. All data of ground surface vibration are shown in Fig. 4 to Fig. 6. Figure 4 represents these vibrations in time history with pile installing into four different soil layers (*i.e.* Soil 1–Soil 4) with the receiver located at 2D. In this figure, four curves decay rapidly before t = 12s. After t = 10s, the curves vibrate with amplitude range between -5×10^{-8} to 5×10^{-8} m. They almost overlap among the curves for the Soil 2, 3 and 4, so no distinct characteristics could be identified or compared.

In Fig. 5, the receiver is located at 5D. Obviously, it is away from the source and the influence is decreased. These curves are totally different from Fig. 4 in oscillation pattern. In Fig. 5, the peak occurs at about 4s with amplitude 1.0×10^{-7} m while pile driving into Soil 3. it is the smallest amplitude for curve for Soil 1. Actually, there is little difference of the peak values among the curves for Soil 2 and 3. Obviously, the source effect is decreased. As regards to the receiver located at 10D, the results show in Fig. 6. The source effect is the lowest and four curves have agreements in time domain. Obviously, the curve for Soil 3 shows the largest vibration amplitude, the second one is the curve for Soil 4, and then curve for Soil 2. The curve for Soil 1 shows the smallest vibration amplitude. Herein, it can be found that the peak amplitude is getting larger as the distance d is increasing. In addition, the soil stiffness affects the simulated result, especially for Soil 3. It is a softer soil layer (*i.e.* smaller stiffness) than both the upper and lower soil layers. Such soil deposits amplify the vibration amplitude when the receiver is getting far away from the source in time domain than the others.

5. CONCLUSIONS

A hybrid method, coupled FEM/SBFEM model, has been developed to predict ground vibrations due to impact pile driving. Using a subdomain formulation, a linear model for dynamic

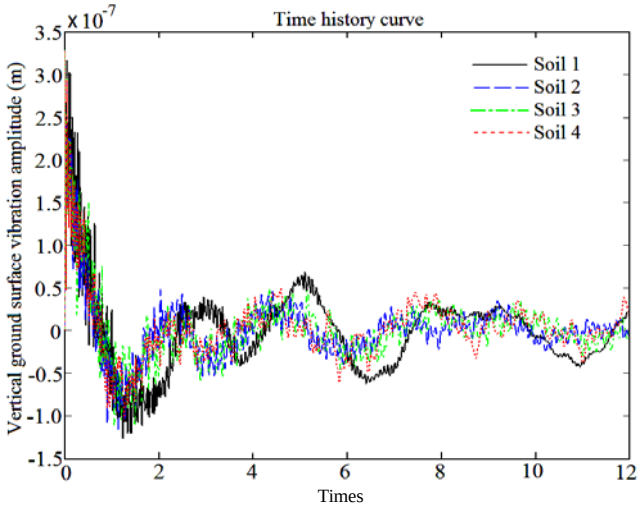

Fig. 4 The vertical displacement on the ground surface away from the pile centre 2D

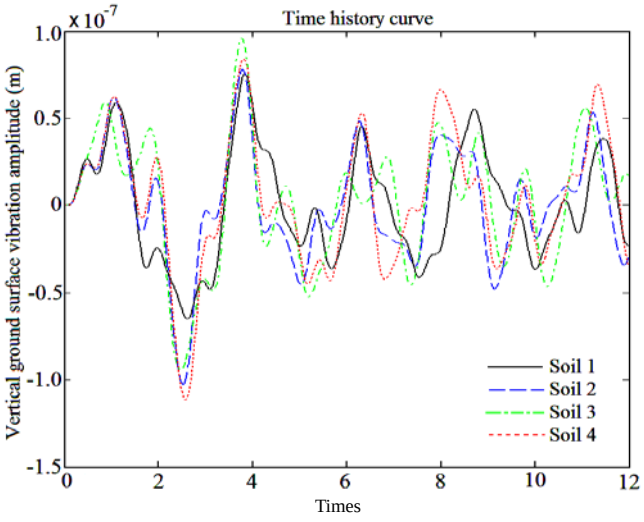

Fig. 5 The vertical displacement on the ground surface away from the pile centre 5D

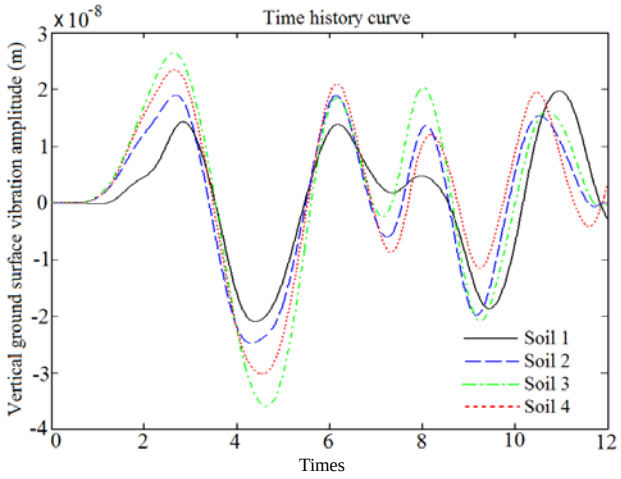

Fig. 6 The vertical displacement on the ground surface away from the pile centre 10D

soil-pile interaction has been implemented. Both pile and surrounding soil (or near-field) is modeled using the finite element method. The soil (or far-field) is modeled as a horizontally layered elastic half space using a boundary element method. The characteristics of the propagating waves on the ground surface have been investigated. Obviously, such numerical model raises the efficiency of numerical simulation and it also avoids the reduction in accuracy by the reflection wave from the artificial boundary. Some results of the pile driving process can be drawn as below:

1. The factor of distance between source to the receiver affects the vibrations seriously. The distance is farther and the curve amplitude is smaller in time domain. In the model with layered soils, the ground surface vibration will not be affected when the receiver is located away from the source more than five times of pile diameter during piling.
2. The soil stiffness affects the ground surface vibration greatly especially when the pile driving depth is into the soft soil layer which is embedded between two harder layers, and then it will produce the maximum vibration amplitude on the ground surface.

REFERENCES

Bettess, P. (1992). *Infinite Elements*. Penshaw Press, Sunderland.

Crouch, R. S. and Bennet, T. (2000). "Efficient EBE treatment of the dynamic far-field in non-linear FE soil-structure interaction analyses." *Proceedings of European Congress on Computational Methods in Applied Sciences and Engineering*, ECCOMAS: Barcelona.

Hilber, H. M., Hughes, T. J. R., and Taylor, R. M. (1997). "Improved numerical dissipation for time integration algorithms in structural dynamics." *Earthquake Engineering and Structural Dynamics*, **5**, 283–292.

Kim, D. S. and Lee, J. S. (2000). "Propagation and attenuation characteristics of various ground vibrations." *Soil Dynamics and Earthquake Engineering*, **19**(2), 115–126.

Lehmann, L., Antes, H., and Schanz, M. (2004). "Transient analysis of soil-structure interaction problems: An effective FEM/SBFEM approach." *Advanced Numerical Analyses of Solids and Structures, and Beyond*, Craz, Austria Institute for Structural Analysis, 99–116.

Lehmann, L. (2005). "An effective finite element approach for soil-structure analysis in time-domain." *Structural Engineering and Mechanics*, **21**(4), 437–450.

Mabsout, E. M. (1999). "Pile driving by numerical cavity expansion." *International Journal for Numerical and Analytical Methods*, **23**(11), 1121–1140.

Ni, S. H., and Chuang, M. J. (2001). "The study of the behavior of bored piles subjected to lateral loading." *Journal of the Chinese Institute of Civil and Hydraulic Engineering*, **13**(2), 178–183. (in Chinese)

Ramshaw, C. L. and Selby, A. R. (2003). *Numerical Analysis and Modelling in Geomechanics-Computational Modelling of Ground Waves Due to Pile Driving*, Spon Press, 129–164.

To, P. and Smith, I. M. (1988). "A note on finite element simulations of pile driving." *International Journal for Numerical and Analytical Methods*, **12**(2), 213–219.

Wolf, J. P. and Song, Ch. (1996). *Finite-Element Modeling of Unbounded Media*. Wiley, England.

Wolf, J. P. and Song, Ch. (2000). "The scaled boundary finite element - a primer: Derivations." *Computer and Structures*, **78**, 211–225.

Wolf, J. P. (2003). *The Scaled Boundary Finite Element Method*. Wiley, England.